Flavor changing effects on single charged Higgs boson production associated with a bottom-charm pair at CERN Large Hadron Collider

Sun Hao, Ma Wen-Gan, Zhang Ren-You, Guo Lei, Han Liang, and Jiang Yi

Department of Modern Physics, University of Science and Technology of China (USTC), Hefei, Anhui 230026, People's Republic of China

(Received 29 January 2007; published 4 May 2007)

We study flavor changing effects on the $pp \to bcH^{\pm} + X$ process at the Large Hadron Collider, which are inspired by the left-handed up-type squark mixings in the minimal supersymmetric standard model (MSSM). We find that the SUSY QCD radiative corrections to $bcH^{\pm}$ coupling can significantly enhance the cross sections at the tree level by a factor about $1.5 \sim 5$ with our choice of parameters. We conclude that the squark-mixing mechanism in the MSSM makes the $pp \to bcH^{\pm} + X$ process a new channel for discovering a charged Higgs boson and investigating flavor changing effects.

DOI: 10.1103/PhysRevD.75.095006 PACS numbers: 12.60.Jv, 14.65.Fy, 14.80.Cp

I. INTRODUCTION

As we know there are stringent experimental constraints against the existence of tree-level flavor changing scalar interactions for light quarks. It leads to the suppression of the flavor changing neutral current (FCNC) couplings at the lowest order. This also is an important feature of the standard model (SM) [1]. Even the 1-loop flavor changing effect in the SM is still small, due to the suppression of the Glashow-Iliopulos-Maiani mechanism [2]. In extension models beyond the SM when new nonstandard particles exist in the loops, significant contributions to flavor changing transitions may appear. Among various new physics models, the minimal supersymmetric extension (MSSM) [3] is widely considered as one of the most appealing extensions of the SM. The MSSM not only can explain the existing experimental data as the SM does, but it also can be used to solve various theoretical problems in the SM, such as the huge hierarchy problem between the electroweak symmetry breaking and the grand unification scales. In the MSSM there exist two Higgs doublets to break the electroweak symmetry. After symmetry breaking, there are five physical Higgs bosons: two CP-even Higgs bosons (h^0, H^0), one CP-odd boson (A^0), and two charged Higgs bosons ($H^{\pm}$) [4]. A significant difference exists between the couplings involving Higgs bosons in the MSSM and those in the SM. In SUSY models, an important feature is that the fermion-Higgs couplings are no longer strictly proportional only to the corresponding mass as they are in the SM. For example, the b-quark coupling with neutral Higgs boson A^0 in the MSSM becomes enhanced for large $\tan\beta = v_2/v_1$, the ratio of the two vacuum expectation values [4]. Thus, different features can be presented due to the existence of the five Higgs bosons in the MSSM which might lead different coupling strengths, decay widths, and production cross sections compared with in the SM.

The understanding of the flavor sector is a major challenge for various extension models of the SM. In the MSSM, the minimal flavor violation is realized by the Cabibbo-Kobayashi-Maskawa (CKM) quark-mixing matrix [5]. While in the general MSSM with flavor violation, a possible flavor mixing between the three sfermion generations are allowed and lead to flavor changing effects. The flavor changing effects originating from such sfermion mixing scenarios normally cannot be generated at the tree level but could show up at the 1-loop level and induce significant contributions to be observed in specific regions of the MSSM parameters.

Searching for scalar Higgs bosons is one of the major objectives of present and future high-energy experiments. In most extensions of the SM, the mass of a charged Higgs boson ($m_{H^{\pm}}$) is predicted to be around the weak scale. However, the Higgs bosons have not been directly explored experimentally until now. At hadron colliders, such as the Fermilab Tevatron and the CERN Large Hadron Collider (LHC), a light charged Higgs boson can be produced from the decay of top quark via $t \to H^+ b$, if $m_{H^{\pm}} < m_t - m_b$ [6]. Otherwise, if the charged Higgs boson is heavier than the top quark, there are four major channels to search for charged Higgs bosons: (1) charged Higgs boson pair production [7–9]; (2) associated production of a charged Higgs boson with a W boson [10]; (3) associated production of a charged Higgs boson with a top quark $gb \to tH^-$ [11]; (4) single charged Higgs production $\bar{c}s$, $\bar{c}b \to H^-$ [12]. The decay of the charged Higgs boson has two major channels: $H^- \to \bar{t}b$ [13] and $H^- \to \tau^- \bar{\nu}$ [14]. At the LHC, the most promising channel to search for the charged Higgs boson in some specific parameter space is $pp \to btH^{\pm} + X$, whose QCD corrections have been studied in Refs. [15–17]. The $pp \to bcH^{\pm} + X$ process is another important alternative channel especially considering the contributions from squark-gluino loops with flavor mixing structure. Diaz-Cruz *et al.* analyzed SUSY radiative corrections to the $bcH^{\pm}$ and tch^0 couplings including squark-mixing effects and showed that these couplings can reveal exciting new discovery channels for the Higgs boson signals at the Tevatron and the LHC [12]. He *et al.* studied the single charged Higgs production process at linear colliders, such

as $e^- e^+ \to b\bar{c}H^+$, $\tau\bar{\nu}H^+$ and $\gamma\gamma \to b\bar{c}H^+$, $\tau\bar{\nu}H^+$ [18]. The flavor changing effect on the neutral Higgs boson production associated with a bottom-strange quark pair in the MSSM at the linear collider was studied in Ref. [19].

As we know, among the three generations of fermions, the top quark is the heaviest one with its mass as high as the electroweak scale. The large top quark mass will enhance the flavor changing Yukawa coupling $bcH^\pm$ at the loop level and make the single charged Higgs production process $pp \to bcH^\pm + X$ to be an important channel for probing flavor violation and searching for charged Higgs boson at hadron colliders. Furthermore, when the neutral scalar (ϕ^0) and the charged scalar ($\phi^\pm$) form a SU(2) doublet, the weak isospin symmetry connects the flavor changing neutral current $tc\phi^0$ to the flavor mixing charged coupling (FMCC) $bc\phi^\pm$ through the (s)quark mixing matrix. Therefore, if we can directly measure the coupling of FMCC at future high energy colliders, it would provide the detailed information on the FCNC and may give more precise constraints on the FCNC than that inferred from kaon and bottom physics obtained from low-energy experiments.

Although the electroweak corrections can contribute to the flavor changing effect on the process $pp \to bcH^\pm + X$, the SUSY QCD corrections via squark-gluino loops are dominant over the previous ones, at least one order larger in magnitude. In this work, we calculate the single charged Higgs boson production process associated with a bottom-charm pair $pp \to bcH^\pm + X$ in the MSSM with left-handed up-type squark mixings at QCD 1-loop level at the CERN LHC. We shall show the importance of squark mixings in the enhancement of production rate for $pp \to bcH^\pm + X$ process. We analyze the SUSY QCD radiative contributions to the process $pp \to bcH^\pm + X$ by adopting the relevant MSSM parameters at the Snowmass point SPS 4 with large $\tan\beta$.

The paper is organized as follows: In Sec. II we present a brief outline on the up-type squark mass matrix considering the left-handed up-type squark mixings and diagonalize it to obtain the mass eigenstates matrix of squarks. In Sec. III, we give the calculations of the cross sections of $pp \to \bar{b}cH^- + X$ up to the order $\mathcal{O}(gg_s^4)$ in the MSSM. The numerical results and discussions are presented in Sec. IV. Finally, a short summary is given.

II. LEFT-HANDED UP-TYPE SQUARK MIXING

In the supersymmetric models, the SM flavor mixings between quarks of three generations can be extended to include the superpartners of quarks and leptons by introducing the supersymmetry soft-breaking mechanism. These models leave further puzzles to the flavor physics, since the soft-breaking Lagrangian of the supersymmetry, which gives a mass spectrum of the supersymmetric particles, involves numerous unconstrained free parameters. In order to fit with low-energy FCNC data, we have to make specific assumptions to these free parameters.

In the study of the $bcH^\pm$ production at hadron colliders, only the flavor mixing in the squark sector is concerned. For the down-type squark mixings, there are possible strong constraints on the mixing parameters from the low-energy experimental data. For example, the mechanism with down-type squark mixings in large $\tan\beta$ could enhance the FCNC B decays by several orders [20] and seems to be ruled out by B-factory experiments. But the up-type squark mixing between $\tilde{t}$ and $\tilde{c}$ is subject to no strong low-energy constraint [21]. Such $\tilde{t}$-$\tilde{c}$ squark mixing is well motivated in low-energy supergravity models [22]. Reference [23] shows that at low energy the $\tilde{t}$-$\tilde{c}$ mixing may be significant due to very heavy top quark, and the mixing between $\tilde{t}_L$ and $\tilde{c}_L$ is most likely to be large, which is proportional to a sum of some soft masses. For theoretical simplicity in this work, we focus on the MSSM with the squark-mixing assumption that only the left-handed up-type squarks in three generations can mix with each other [24]. In the super CKM basis $\tilde{U}' = (\tilde{u}_L, \tilde{u}_R, \tilde{c}_L, \tilde{c}_R, \tilde{t}_L, \tilde{t}_R)$, the 6×6 squark mass matrix $\mathcal{M}^2_{\tilde{U}}$ of up-type squark sector takes the form as [25]

$$\mathcal{M}^{\,2}_{\tilde{U}} = \begin{pmatrix} M^2_{L,u} & a_u m_u & \lambda_{12} M_{L,u} M_{L,c} & 0 & \lambda^*_{31} M_{L,u} M_{L,t} & 0 \\ a^*_u m_u & M^2_{R,u} & 0 & 0 & 0 & 0 \\ \lambda^*_{12} M_{L,c} M_{L,u} & 0 & M^2_{L,c} & a_c m_c & \lambda_{23} M_{L,c} M_{L,t} & 0 \\ 0 & 0 & a^*_c m_c & M^2_{R,c} & 0 & 0 \\ \lambda_{31} M_{L,t} M_{L,u} & 0 & \lambda^*_{23} M_{L,t} M_{L,c} & 0 & M^2_{L,t} & a_t m_t \\ 0 & 0 & 0 & 0 & a^*_t m_t & M^2_{R,t} \end{pmatrix}, \tag{2.1}$$

where

$$\begin{aligned} M^2_{L,q} &= M^2_{\tilde{Q},q} + m^2_Z \cos 2\beta \left(\frac{1}{2} - Q_q \sin^2\theta_W\right) + m^2_q, \\ M^2_{R,q} &= M^2_{\tilde{U},q} + Q_q m^2_Z \cos 2\beta \sin^2\theta_W + m^2_q, \\ a_q &= A_q - \mu \cot\beta, \qquad (q = u, c, t). \end{aligned} \tag{2.2}$$

with m_Z being the mass of Z^0, and m_q, Q_q the up-quark mass and charge. $M_{\tilde{Q},q}$ and $M_{\tilde{U},q}$ are mass parameters of supersymmetry soft breaking. $A_q (q = u, c, t)$ are the trilinear scalar coupling parameters of Higgs boson with two scalar quarks. μ is the mass parameter of the Higgs boson sector and $\tan\beta$ is the ratio of the vacuum expectation values in this sector. $\sin\theta_W$ contains the electroweak mix-

ing angle θ_W. λ_{12}, λ_{23}, and λ_{31} are the flavor mixing strengths of the $\tilde{u}_L$–$\tilde{c}_L$, $\tilde{c}_L$–$\tilde{t}_L$, and $\tilde{t}_L$–$\tilde{u}_L$ sectors, respectively. Since we do not consider the CP violation, all these squark-mixing parameters have real and positive values varying in the range of [0, 1].

To obtain the mass eigenstates of the up-type squarks, we should introduce a unitary matrix $\mathcal{R}^{(U)}$ defined as

$$\tilde{U}' = \mathcal{R}^{(U)}\tilde{U}, \tag{2.3}$$

where

$$\tilde{U}' = \begin{pmatrix} \tilde{u}_L \\ \tilde{u}_R \\ \tilde{c}_L \\ \tilde{c}_R \\ \tilde{t}_L \\ \tilde{t}_R \end{pmatrix}, \qquad \tilde{U} = \begin{pmatrix} \tilde{u}_1 \\ \tilde{u}_2 \\ \tilde{u}_3 \\ \tilde{u}_4 \\ \tilde{u}_5 \\ \tilde{u}_6 \end{pmatrix} = \begin{pmatrix} \tilde{u}_1 \\ \tilde{u}_2 \\ \tilde{c}_1 \\ \tilde{c}_2 \\ \tilde{t}_1 \\ \tilde{t}_2 \end{pmatrix}. \tag{2.4}$$

The up-squark mass matrix $M^2_{\tilde{U}}$ is diagonalized by the 6×6 matrix $\mathcal{R}^{(U)}$ via

$$\mathcal{R}^{(U)\dagger}\mathcal{M}^2_{\tilde{U}}\mathcal{R}^{(U)} = \mathrm{diag}\{m^2_{\tilde{u}_1}, \ldots, m^2_{\tilde{u}_6}\}, \tag{2.5}$$

where $m^2_{\tilde{u}_j}(j = 1, \ldots, 6)$ are the masses of mass eigenstates of the six up-type squarks which depend on λ_{12}, λ_{23}, and λ_{31}.

III. CALCULATION OF THE PROCESS $pp \to bcH^{\pm} + X$

The exclusive process of single charged Higgs boson production associated with a bottom-charm quark pair, $pp \to bcH^{\pm} + X$, involves the contributions from the subprocesses of $q\bar{q}(q = u, d, c, s)$ annihilation and gluon-gluon fusion. Since the processes $q\bar{q}/gg \to b\bar{c}H^+$ have the same total and differential cross sections as their corresponding charge-conjugate subprocesses $q\bar{q}/gg \to \bar{b}cH^-$ in the CP-conserving MSSM, we present here only the calculations of the process $pp \to \bar{b}cH^- + X$. For each subprocesses of $q\bar{q} \to \bar{b}cH^-$ and $gg \to \bar{b}cH^-$, we depict one tree-level [$\mathcal{O}(gg_s^2)$] Feynman diagram as a demonstration in Figs. 1(a) and 1(b), respectively.

The tree-level total cross section of $pp \to \bar{b}cH^- + X$ can be obtained by doing the following integration:

$$\sigma_{\mathrm{tree}}(pp(AB) \to \bar{b}cH^- + X) = \sum_{ij=u\bar{u},d\bar{d}}^{s\bar{s},c\bar{c},gg} \frac{1}{1+\delta_{ij}} \int dx_A dx_B [G_{i/A}(x_A, \mu_f) G_{j/B}(x_B, \mu_f) \hat{\sigma}^{ij}_{\mathrm{tree}}(x_A, x_B, \mu_f) + (A \leftrightarrow B)], \tag{3.1}$$

where x_A and x_B are defined as

$$x_A = \frac{p_1}{P_A}, \qquad x_B = \frac{p_2}{P_B}, \tag{3.2}$$

where A and B represent the incoming colliding protons. p_1, p_2, P_A, and P_B are the momenta of partons and protons. $\hat{\sigma}^{ij}_{\mathrm{tree}}(ij = u\bar{u}, d\bar{d}, c\bar{c}, s\bar{s}, gg)$ is the total leading-order (LO) cross section at parton level for incoming i and j partons. $G_{i/A(B)}$ is the LO parton distribution function for parton i in hadron $A(B)$. We adopt CTEQ6L1 parton distribution function in the calculation of the tree-level cross section [26].

In the calculation of the SUSY QCD next-to-leading order (NLO) contributions in the framework of the MSSM with left-handed up-type squark mixings, we adopt the 't Hooft-Feynman gauge, and use dimensional regularization method in $D = 4 - 2\epsilon$ dimensions to isolate the ultraviolet (UV), soft and collinear infrared (IR) singularities. The modified minimal subtraction ($\overline{\mathrm{MS}}$) scheme is employed to renormalize and eliminate UV divergency. The SUSY QCD NLO contributions can be divided into two parts: the virtual contributions from 1-loop diagrams and the real gluon/light-quark emission contributions.

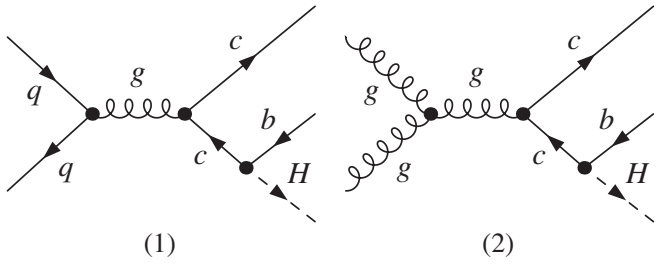

FIG. 1. (1) One of the tree-level [$\mathcal{O}(gg_s^2)$] Feynman diagrams for $q\bar{q} \to \bar{b}cH^-$ subprocess. (2) One of the tree-level [$\mathcal{O}(gg_s^2)$] Feynman diagrams for $gg \to \bar{b}cH^-$ subprocess.

The unrenormalized virtual contribution to the subprocess $q\bar{q}/gg \to \bar{b}cH^-$ in the MSSM consists of self-energy, vertex, box, and pentagon diagrams. These 1-loop diagrams for subprocess $q\bar{q}/gg \to \bar{b}cH^-$ can be divided into two parts: one is the SM-like part which comprises the diagrams including gluon/quark loops; another is the SUSY part involving virtual gluino/squark exchange loops. In the latter part, contributions from the 1-loop diagrams with left-handed up-type squark mixings between different generations are considered. For demonstration, we plot the QCD 1-loop pentagon diagrams for the $gg \to b\bar{c}H^+$ subprocess in Fig. 2. The figures of Fig. f2(1) belongs to the SM-like part, while Fig. f2(2) to the SUSY part. The amplitude for the virtual SM-like contribution part contains both UV and soft/collinear IR singularities, while the amplitude corresponding to the SUSY loop part contains only UV singularities. In order to remove the UV divergences, we renormalize the relevant fields, the masses of

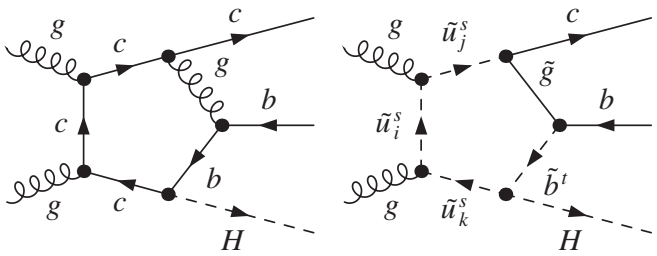

FIG. 2. The representative QCD pentagon Feynman diagrams for $gg \to \bar{b}cH^-$ subprocess. (1) is the SM-like diagram, and (2) is the SUSY QCD 1-loop diagram. The lower-index i in $\tilde{q}_i^s$ implies the ith generation ($i = 1, 2, 3$) and the upper-index $s = 1, 2$.

charm quark and bottom quark in propagators and the $bcH^\pm$ Yukawa coupling by adopting an on shell (OS) scheme. The renormalization constants of the CKM matrix elements $V_{ij}(i, j = 1, 2, 3)$ can be obtained by keeping the unitarity of the renormalized CKM matrix, expressed as [27]

$$\delta V_{ij} = \tfrac{1}{4}[(\delta Z_{ik}^{u,L} - \delta Z_{ik}^{u,L\dagger})V_{kj} - V_{ik}(\delta Z_{kj}^{d,L} - \delta Z_{kj}^{d,L,\dagger})]. \tag{3.3}$$

We use the $\overline{\rm MS}$ mass of the bottom quark $[\bar{m}_b(\mu_r)]$ in a $bcH^\pm$ Yukawa coupling to absorb the large logarithms contributions which arise from the renormalization of bottom quark mass [28], but we keep the bottom quark pole mass everywhere else. The bottom quark mass in the propagator is renormalized by adopting the OS scheme. The expressions of the $\overline{\rm MS}$ mass of the bottom quark $\bar{m}_b(\mu_r)$ corresponding 1-loop and 2-loop renoramlization groups are given by

$$\bar{m}_b(\mu_r)_{\text{1-loop}} = m_b\left[\frac{\alpha_s(\mu_r)}{\alpha_s(m_b)}\right]^{c_0/b_0}, \tag{3.4}$$

$$\bar{m}_b(\mu_r)_{\text{2-loop}} = m_b\left[\frac{\alpha_s(\mu_r)}{\alpha_s(m_b)}\right]^{c_0/b_0}\left[1 + \frac{c_0}{b_0}(c_1 - b_1) \times \frac{\alpha_s(\mu_r) - \alpha_s(m_b)}{\pi}\right]\left(1 - \frac{4}{3}\frac{\alpha_s(m_b)}{\pi}\right), \tag{3.5}$$

where

$$b_0 = \frac{1}{4\pi}\left(\frac{11}{3}N_c - \frac{2}{3}n_f\right), \qquad c_0 = \frac{1}{\pi},$$
$$b_1 = \frac{1}{2\pi}\frac{51N_c - 19n_f}{11N_c - 2n_f}, \qquad c_1 = \frac{1}{72\pi}(101N_c - 10n_f) \tag{3.6}$$

In our calculation we adopt $\bar{m}_b(\mu_r)_{\text{1-loop}}$ in Eq. (3.4) and $\bar{m}_b(\mu_r)_{\text{2-loop}}$ in Eq. (3.5) as the $\bar{m}_b(\mu_r)$ mass for the LO and NLO cross sections, respectively [29]. The renormalization of the bottom quark mass in the Yukawa coupling is defined as

$$m_b^0 = \bar{m}_b(\mu_r)[1 + \delta^{\text{SM-like}} + \delta^{\text{SUSY}}], \tag{3.7}$$

where the counterterm of the SM-like QCD part $\delta^{\text{SM-like}}$ is calculated in $\overline{\rm MS}$ scheme, while SUSY counterterm part δ^{SUSY} is calculated in the OS scheme. Because of the fact that there are significant corrections to $bcH^\pm$ coupling for large value of $\tan\beta$, we absorb these corrections in the Yukawa coupling [30]. The resummed $bcH^\pm$ Yukawa coupling can be expressed as [17,28,31]

$$g_{\bar{b}cH^-} = \frac{igV_{cb}}{\sqrt{2}m_W}\left\{m_c \cot\beta P_R + \bar{m}_b(\mu_r)\frac{1 - \frac{\Delta_b}{\tan^2\beta}}{1 - \Delta_b}\tan\beta P_L\right\}, \tag{3.8}$$

where

$$\begin{aligned}
\Delta_b &= \frac{\Delta m_b}{1 + \Delta_1}, \\
\Delta m_b &= \frac{2}{3}\frac{\alpha_s}{\pi}m_{\tilde{g}}\mu\tan\beta I(m_{\tilde{b}_3}^2, m_{\tilde{b}_2}^2, m_{\tilde{g}}^2), \\
\Delta_1 &= -\frac{2}{3}\frac{\alpha_s}{\pi}m_{\tilde{g}}A_b I(m_{\tilde{b}_1}^2, m_{\tilde{b}_2}^2, m_{\tilde{g}}^2), \\
I(a, b, c) &= -\frac{ab\log\frac{a}{b} + bc\log\frac{bc}{a} + ca\log\frac{c}{a}}{(a - b)(b - c)(c - a)}.
\end{aligned} \tag{3.9}$$

Since in the calculation of the cross section of the process $pp \to \bar{b}cH^- + X$ at the tree level, we used the resummed $bcH^\pm$ Yukawa coupling, we have to add a finite renormalization of the bottom quark mass in the $bcH^\pm$ Yukawa coupling to avoid double counting in the SUSY QCD NLO corrections to the cross section [32]:

$$m_b \to \bar{m}_b(\mu_r)[1 + \Delta_b^{H^-}] + O(\alpha_s^2), \tag{3.10}$$

$$\Delta_b^{H^-} = \frac{2}{3}\frac{\alpha_s}{\pi}\left(1 + \frac{1}{\tan^2\beta}\right)m_{\tilde{g}}\mu\tan\beta I(m_{\tilde{b}_1}^2, m_{\tilde{b}_2}^2, m_{\tilde{g}}^2). \tag{3.11}$$

For the renormalization of the strong coupling constant g_s, we divide the counterterm of the strong coupling constant into two terms: SM-like QCD term and SUSY term $[\delta g_s = \delta g_s^{(\text{SM-like})} + \delta g_s^{(\text{SUSY})}]$, and the explicit expressions of these two terms can be obtained by adopting $\overline{\rm MS}$ scheme at renormalization scale μ_r [17,33]:

$$\frac{\delta g_s^{(\text{SM-like})}}{g_s} = -\frac{\alpha_s(\mu_r)}{4\pi}\left[\frac{\beta_0^{(\text{SM-like})}}{2}\frac{1}{\bar{\epsilon}} + \frac{1}{3}\ln\frac{m_t^2}{\mu_r^2}\right], \tag{3.12}$$

$$\frac{\delta g_s^{(\mathrm{SUSY})}}{g_s} = -\frac{\alpha_s(\mu_r)}{4\pi}\left[\frac{\beta_0^{(\mathrm{SQCD})}}{2}\frac{1}{\bar{\epsilon}} + \frac{N_c}{3}\ln\frac{m_{\tilde{g}}^2}{\mu_r^2} + \sum_{U=u,c,t}^{i=1,2}\frac{1}{12}\ln\frac{m_{\tilde{U}_i}^2}{\mu_r^2} + \sum_{D=d,s,b}^{j=1,2}\frac{1}{12}\ln\frac{m_{\tilde{D}_j}^2}{\mu_r^2}\right], \tag{3.13}$$

where we have used the notations

$$\begin{aligned}\beta_0^{(\text{SM-like})} &= \tfrac{11}{3}N_c - \tfrac{2}{3}n_f - \tfrac{2}{3},\\ \beta_0^{(\mathrm{SUSY})} &= -\tfrac{2}{3}N_c - \tfrac{1}{3}(n_f+1).\end{aligned} \tag{3.14}$$

The number of colors N_c equals 3, the number of active flavors is taken to be $n_f = 5$ and $1/\bar{\epsilon} = 1/\epsilon_{UV} - \gamma_E + \ln(4\pi)$. The summation is taken over the indexes of squarks and generations. Since the $\overline{\mathrm{MS}}$ scheme violates supersymmetry, it is necessary that the $q\tilde{q}\,\tilde{g}$ Yukawa coupling $\hat{g}_s$, which should be the same with the qqg gauge coupling g_s in the supersymmetry, takes a finite shift at 1-loop order as shown in Eq. (3.15) [34]:

$$\hat{g}_s = g_s\left[1 + \frac{\alpha_s}{8\pi}\left(\frac{4}{3}N_c - C_F\right)\right], \tag{3.15}$$

with $C_F = 4/3$. In our numerical calculation we take this shift between $\hat{g}_s$ and g_s into account.

The SUSY QCD 1-loop Feynman diagrams for both $q\bar{q} \to \bar{b}cH^-$ and $gg \to \bar{b}cH^-$ subprocesses can be divided into virtual gluon/quark exchange part (SM-like) and virtual gluino/squark exchange part (SUSY). We express the renormalized amplitudes for both subprocesses as

$$M_{\mathrm{virtual}}^{q\bar{q},gg} = M_{\text{SM-like}}^{q\bar{q},gg} + M_{\mathrm{SUSY}}^{q\bar{q},gg}. \tag{3.16}$$

Then the SUSY QCD NLO contributions to the cross sections of the subprocesses $q\bar{q}/gg \to \bar{b}cH^-$ can be expressed as

$$\hat{\sigma}_{\mathrm{virtual}}^{q\bar{q},gg} = \int d\Phi_3 \overline{\sum}(2\,\mathrm{Re}(M_{\mathrm{tree}}^{q\bar{q},gg} M_{\mathrm{virtual}}^{q\bar{q},gg\dagger}) + |M_{\mathrm{tree}}^{q\bar{q},gg}|^2), \tag{3.17}$$

where $d\Phi_3$ is a three-body phase space element, $M_{\mathrm{tree}}^{q\bar{q}}$ and M_{tree}^{gg} are the Born amplitudes for $q\bar{q}/gg \to \bar{b}cH^-$ subprocesses separately, and $M_{\mathrm{virtual}}^{q\bar{q}}$ and $M_{\mathrm{virtual}}^{gg}$ are their renormalized amplitudes of the SUSY QCD 1-loop diagrams. The bar over the summation in Eq. (3.17) recalls averaging over initial spin and color states.

$\hat{\sigma}_{\mathrm{virtual}}^{q\bar{q},gg}$ are free of UV divergences but contain soft/collinear IR divergences, among them the soft IR divergence can be cancelled by adding with the soft real gluon emission corrections. The soft and collinear singularities from real gluon emission subprocess can be conveniently isolated by slicing the phase space into different regions defined with suitable cutoffs [35]. We introduce an arbitrary soft cutoff $\delta_s (\equiv 2E_g/\sqrt{\hat{s}})$ with small value to separate the phase space of the gluon emission $2 \to 4$ subprocess into two regions, i.e., soft- and hard-gluon emission regions. Then for the gluon emission $2 \to 4$ subprocesses based on $(q\bar{q}, q'\bar{q}', gg) \to \bar{b}cH^-$ ($q = u, d, q' = s, c$), we have

$$\begin{aligned}\hat{\sigma}_{\mathrm{real}}((q\bar{q}, q'\bar{q}', gg) \to \bar{b}cH^- g) &= \hat{\sigma}_{\mathrm{soft}}((q\bar{q}, q'\bar{q}', gg) \to \bar{b}cH^- g)\\ &\quad + \hat{\sigma}_{\mathrm{hard}}((q\bar{q}, q'\bar{q}', gg) \to \bar{b}cH^- g),\end{aligned} \tag{3.18}$$

where $\hat{\sigma}_{\mathrm{soft}}$ is obtained by integrating over the soft region of the emitted gluon phase space and contains all the soft IR singularities. Furthermore, we decompose each cross section of $\hat{\sigma}_{\mathrm{hard}}$ for hard-gluon emission subprocesses $q\bar{q}/q'\bar{q}'/gg \to \bar{b}cH^- g$ and light-quark emission subprocesses $\hat{\sigma}_{\mathrm{real}}$ for $(\bar{q}g, qg) \to \bar{b}cH^-(\bar{q}, q)$, into a sum of collinear and noncollinear terms to isolate the remaining collinear singularities from $\hat{\sigma}_{\mathrm{hard}}$ and $\hat{\sigma}_{\mathrm{real}}$, by introducing another cutoff δ_c called collinear cutoff.

The cross sections in the noncollinear hard-gluon/light-quark emission regions can be obtained by performing the phase space integration in four dimensions by using the Monte Carlo method. Then we get the SUSY QCD NLO corrected cross sections for subprocesses $q\bar{q}/q'\bar{q}'/gg \to \bar{b}cH^-$ as follows. For $q\bar{q}$ annihilation ($q = u, d$) subprocesses,

$$\begin{aligned}\hat{\sigma}_{\mathrm{loop}}(q\bar{q} \to \bar{b}cH^-) &= \hat{\sigma}_{\mathrm{tree}}(q\bar{q} \to \bar{b}cH^-) + \hat{\sigma}_{\mathrm{virtual}}(q\bar{q} \to \bar{b}cH^-)\\ &\quad + \sum_{ij=q\bar{q},}^{\bar{q}g,qg}\hat{\sigma}_{\mathrm{real}}(ij \to \bar{b}cH^-(g, \bar{q}, q)),\end{aligned} \tag{3.19}$$

while for $q'\bar{q}'$ annihilation ($q' = c, s$) and gg fusion subprocesses,

$$\begin{aligned}\hat{\sigma}_{\mathrm{loop}}(q'\bar{q}'/gg \to \bar{b}cH^-) &= \hat{\sigma}_{\mathrm{tree}}(q'\bar{q}'/gg \to \bar{b}cH^-)\\ &\quad + \hat{\sigma}_{\mathrm{virtual}}(q'\bar{q}'/gg \to \bar{b}cH^-)\\ &\quad + \hat{\sigma}_{\mathrm{real}}(q'\bar{q}'/gg \to \bar{b}cH^- g),\end{aligned} \tag{3.20}$$

The remaining collinear IR divergences in Eqs. (3.19) and (3.20) are absorbed into the parton distribution functions, separately. Then the SUSY QCD NLO corrected total cross section for $pp \to \bar{b}cH^- + X$ process σ_{loop}, can be obtained by using Eq. (3.1) and replacing $\hat{\sigma}_{\mathrm{tree}}^{ij}(ij \to \bar{b}cH^-)$, $(ij = q\bar{q}, q'\bar{q}', gg)$ by $\hat{\sigma}_{\mathrm{loop}}(ij \to \bar{b}cH^-)$, $(ij = q\bar{q}, q'\bar{q}', gg, \bar{q}g, qg)$, and CTEQ6L1 parton distribution functions by CTEQ6M ones [26]. The total cross section $\sigma_{\mathrm{loop}}(pp \to \bar{b}cH^- + X)$ up to SUSY QCD NLO should be independent on the two arbitrary cutoffs δ_s and δ_c. In both our analytical and numerical calculations, we checked the cancellations of the UV and IR divergences and found that the final results are both UV and IR finite.

IV. NUMERICAL RESULTS AND DISCUSSIONS

In this section, we present some numerical results of the total and differential cross sections of the precess $pp \to bcH^{\pm} + X$ inspired by the squark-mixing loop contributions at the LHC. We take the SM parameters as $m_W = 80.425$ GeV, $m_Z = 91.1876$ GeV, $m_t = 175$ GeV, $m_b = 4.7$ GeV, $m_c = 1.2$ GeV, $m_s = 0.15$ GeV, $V_{cb} = 0.04$, $V_{ub} = 0.0035$, $V_{cd} = 0.222$, $V_{cs} = 0.97415$, $V_{cb} = 0.04$, and $V_{tb} = 0.99915$ [36] and neglect the light-quark masses ($m_{u,d}$) in the numerical calculation. The value of the fine structure constant at the energy scale of Z^0 pole mass is taken as $\alpha_{\rm ew}(m_Z)^{-1} = 127.918$ [36]. We use the CTEQ6L1 and CTEQ6M parton distribution functions for the calculations of LO and NLO contributed cross sections, respectively [26]. The colliding energy of the proton-proton collider at the LHC is $\sqrt{s} = 14TeV$. We fix the value of the renormalization/factorization scale being $Q = Q_0 = \mu_r = \mu_f$ for simplicity, where Q_0 is defined to be half of the final particle masses. As a numerical demonstration, we refer to the relevant MSSM parameters of Snowmass point SPS 4 with high $\tan\beta$ [37,38] except considering the left-handed up-type squark mixings in the MSSM. SPS 4 is a point in the minimal supergravity model with input parameters:

$$m_0 = 400 \text{ GeV}, \quad m_{1/2} = 300 \text{ GeV}, \quad A_0 = 0, \quad \tan\beta = 50, \quad \mu > 0. \tag{4.1}$$

Since the squark sector in Snowmass points does not include squark mixing, we do not adopt the SPS 4 physical sparticle spectrum but the ISAJET [39] equivalent input MSSM parameters at this benchmark point, with which one can reproduce the ISAJET spectrum with SUSYGEN [40] and PYTHIA [41]. The relevant MSSM parameters at SPS 4 point we used in our calculation are listed below [38]:

$$\begin{aligned}
\tan\beta &= 50, \\
m_{H^{\pm}} &= 416.28 \text{ GeV}, \\
m_{\tilde{g}} &= 721.03 \text{ GeV}, \\
m_{\tilde{u}_L} &= m_{\tilde{d}_L} = m_{\tilde{c}_L} = m_{\tilde{s}_L} = 732.2 \text{ GeV}, \\
m_{\tilde{b}_L} &= m_{\tilde{t}_L} = 640.09 \text{ GeV}, \\
m_{\tilde{u}_R} &= m_{\tilde{c}_R} = 716.00 \text{ GeV}, \\
m_{\tilde{d}_R} &= m_{\tilde{s}_R} = 713.87 \text{ GeV}, \\
m_{\tilde{b}_R} &= 673.40 \text{ GeV}, \\
m_{\tilde{t}_R} &= 556.76 \text{ GeV}, \\
A_t &= -552.20 \text{ GeV}, \\
A_b &= -729.52 \text{ GeV}.
\end{aligned} \tag{4.2}$$

The squark-mixing parameters λ_{12}, λ_{31}, and λ_{23} are constrained by low-energy data on FCNC [21]. Following Ref. [21], we use the bounds for the squark-mixing parameters as

$$\begin{aligned}
\lambda_{12} &< 0.1\sqrt{m_{\tilde{u}} m_{\tilde{c}}}/500 \text{ GeV}, \\
\lambda_{31} &< 0.098\sqrt{m_{\tilde{u}} m_{\tilde{t}}}/500 \text{ GeV}, \\
\lambda_{23} &< 8.2 m_{\tilde{c}} m_{\tilde{t}}/(500 \text{ GeV})^2.
\end{aligned} \tag{4.3}$$

Considering the above limitations on squark-mixing parameters, in our calculations we use the MSSM parameters shown in Eq. (4.2) and take $\lambda_{12} = 0.03$, $\lambda_{31} = 0.03$, and $\lambda_{23} = \lambda = 0.6$, which satisfy the constraints of Eq. (4.3), if there is no different statement. Actually, our calculation shows that the cross section involving NLO QCD corrections for process $pp \to bcH^{\pm} + X$ is mostly related to the squark-mixing parameter λ_{23}, but not sensitive to the λ_{12} and λ_{31}. That implies the contributions from the $\tilde{u}_L$-$\tilde{c}_L$ and $\tilde{u}_L$-$\tilde{t}_L$ squark mixings are very small in our chosen parameter space.

In numerical calculation, we put the cuts on the transverse momenta of final bottom, charm quarks and charged Higgs bosons as

$$|p_T^b| > 20 \text{ GeV}, \quad |p_T^c| > 20 \text{ GeV}, \quad |p_T^{H^-}| > 10 \text{ GeV}. \tag{4.4}$$

As we discussed in the above section, the final results should be independent on cutoffs δ_s and δ_c. That is also one of the checks of the correctness of our calculation. We checked the independence of cutoffs δ_s and δ_c in our calculation. In the following numerical calculation we fix $\delta_s = 10^{-3}$ and $\delta_c = 10^{-5}$.

In Fig. 3 we present the total cross sections for the process $pp \to bcH^{\pm} + X$ at the tree level ($\sigma_{\rm tree}$) and up

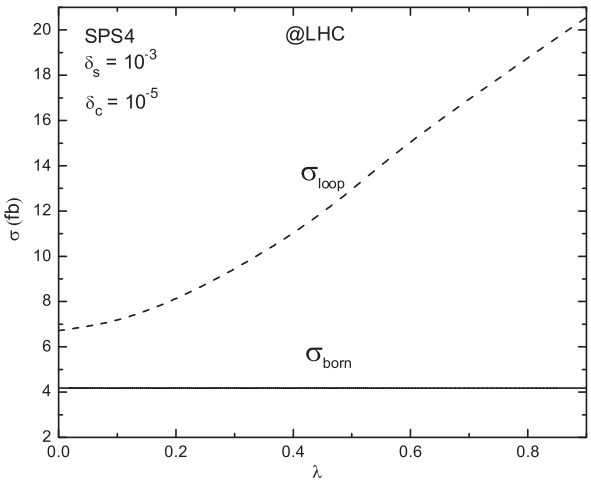

FIG. 3. The cross sections for the process $pp \to bcH^{\pm} + X$ at the tree-level [$\mathcal{O}(gg_s^2)$] $\sigma_{\rm tree}$ and up to QCD 1-loop level [$\mathcal{O}(gg_s^4)$] $\sigma_{\rm loop}$ as the functions of the mixing strength parameter $\lambda(= \lambda_{23})$ in the up-type squark mass matrix at the LHC. The relevant MSSM parameters at the Snowmass point SPS 4 are adopted [shown in Eq. (4.2)].

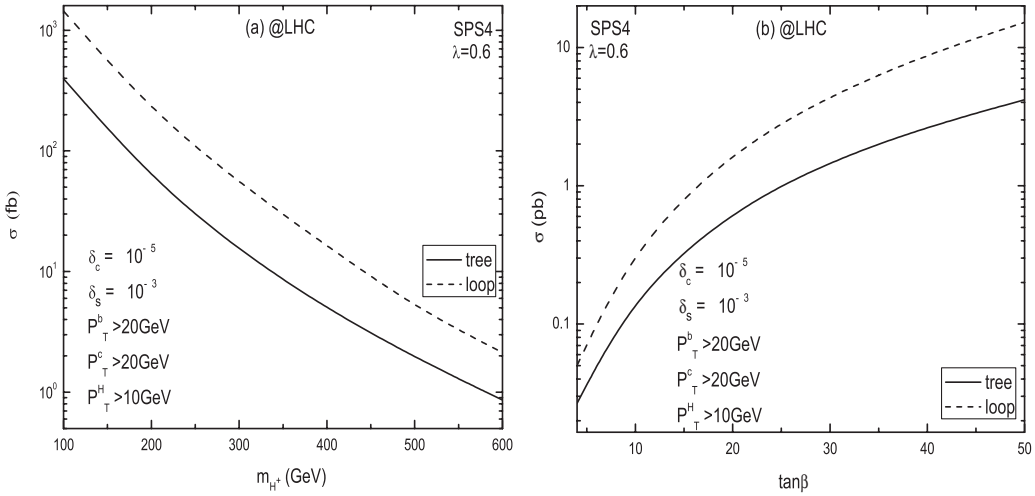

FIG. 4. The cross sections for the process $pp \to bcH^{\pm} + X$ at the tree-level σ_{tree} and up to SUSY QCD NLO σ_{loop} as the functions of the mass of the charged Higgs boson [Fig. 4(a)] and the ratio of the vacuum expectation values $\tan\beta$ [Fig. 4(b)]. The other relevant MSSM parameters are taken from the Snowmass point SPS 4 listed in Eq. (4.2).

to SUSY QCD NLO (σ_{loop}) as the functions of the mixing strength between $\tilde{c}_L$ and $\tilde{t}_L$, $\lambda(=\lambda_{23})$, at the LHC with the relevant MSSM parameters at the Snowmass point SPS 4 shown in Eq. (4.2). We can see the 1-loop correction significantly enhances the corresponding LO cross section (solid curve), and the loop contribution goes up with the increment of the mixing parameter λ. As we know the tree-level cross section for $pp \to bcH^{\pm} + X$ process is suppressed by the CKM matrix element in the Yukawa coupling of $bcH^{\pm}$. But the mixing between $\tilde{c}_L$ and $\tilde{t}_L$ in the SUSY soft-breaking sector can make the 1-loop contributions quite sizable and significantly increases the tree-level cross section by a factor of $1.5 \sim 5$, which is shown in Fig. 3.

In Fig. 4 we depict the cross sections for the process $pp \to bcH^{\pm} + X$ at the tree level and up to SUSY QCD NLO at the LHC as the functions of the mass of charged Higgs boson in Fig. 4(a) and the ratio of the vacuum expectation values $\tan\beta$ in Fig. 4(b), respectively, by taking the other MSSM parameter values from the Snowmass point SPS 4 [see Eq. (4.2)]. We can read from Fig. 4(a) that when $m_{H^{\pm}}$ increases from 100 GeV to 600 GeV, the total NLO QCD cross section decreases from 1.548 pb to 2.13 fb at the LHC, while the tree-level cross section decreases from 0.40 fb to 0.86 fb. We can see that if the MSSM scenario with left-handed up-type squark mixings is really true, the LHC machine with an integrated luminosity of about 100 fb^{-1} can have the potential to find the

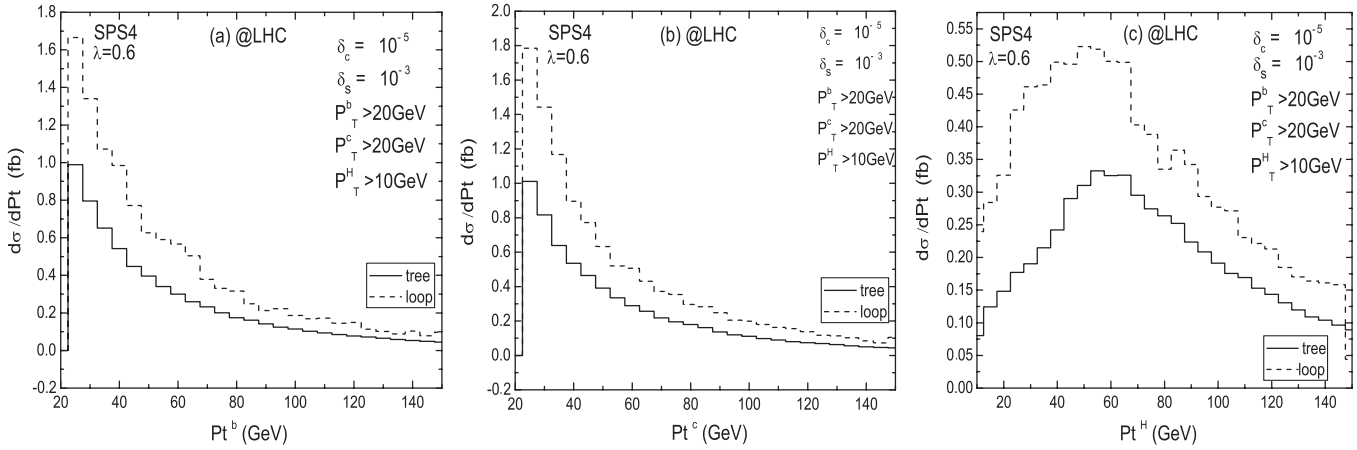

FIG. 5. The differential cross sections of the $pp \to bcH^{\pm} + X$ process at the tree level [$\mathcal{O}(gg_s^2)$] and up to the SUSY QCD NLO [$\mathcal{O}(gg_s^4)$] as the functions of (a) the transverse momentum of bottom quark p_T^b, (b) the transverse momentum of charm quark p_T^c, and (c) the transverse momentum of the charged Higgs boson $p_T^{H^{\pm}}$ at the LHC, with the relevant parameters of the Snowmass point SPS 4 [shown in Eq. (4.2)].

signature of charged Higgs bosons via the process $pp \to bcH^{\pm} + X$ with $m_{H^{\pm}}$ in the range of [100 GeV, 600 GeV]. Figure 4(b) shows that with $m_{H^{\pm}} = 416.28$ GeV the cross section up to the $\mathcal{O}(gg_s^4)$ order σ_{loop} increases from 0.05 fb to 15.18 fb, as $\tan\beta$ varies from 4 to 50, while the tree-level cross section is much smaller than the σ_{loop}. We can conclude that the production rate of the single charged Higgs bosons associated with bottom-charm quark pair at the LHC can be enhanced by the gluino/squark loop contributions in the MSSM with squark-mixing structure.

In Figs. 5(a)–5(c) we present the distributions of the differential cross sections $d\sigma_{\text{tree,loop}}/dp_T^b$, $d\sigma_{\text{tree,loop}}/dp_T^c$, $d\sigma_{\text{tree,loop}}/dp_T^{H^{\pm}}$ for the process $pp \to bcH^{\pm} + X$ in the MSSM with left-handed up-type squark-mixing structure and the relevant parameters at the Snowmass point SPS 4 [shown in Eq. (4.2)] at the LHC. These figures demonstrate that the loop contributions up to the order $[\mathcal{O}(gg_s^4)]$ can significantly enhance the tree-level differential cross sections $d\sigma_{\text{tree}}/dp_T^b$, $d\sigma_{\text{tree}}/dp_T^c$, and $d\sigma_{\text{tree}}/dp_T^{H^{\pm}}$ at the LHC. We find that in the low p_T^b and p_T^c regions the corresponding differential cross section values including SUSY QCD NLO corrections can be very large.

V. SUMMARY

The general three-family up-type squark mass matrix originating from the soft SUSY breaking sector can induce the cross section enhancement for the $pp \to bcH^{\pm} + X$ process at 1-loop level. In this paper we investigated the flavor changing effects on the production of single charged Higgs bosons in association with b-c quark pair in the framework of the MSSM with left-handed up-type squark mixings. We analyzed the dependence of the cross section involving NLO QCD corrections for $pp \to bcH^{\pm} + X$ process on the charged Higgs boson mass $m_{H^{\pm}}$, the ratio of the vacuum expectation values $\tan\beta$, and the distributions of the transverse momenta of bottom quark p_T^b, charm quark p_T^c, and charged Higgs boson $p_T^{H^{\pm}}$ at the CERN LHC. We find that the 1-loop contributions are mostly inspired by the mixing of the $\tilde{c}_L$-$\tilde{t}_L$ sector, and the QCD NLO corrections can significantly enhance the corresponding tree-level $[\mathcal{O}(gg_s^2)]$ cross sections in the MSSM with squark mixings. Our numerical results show the corrected cross section can reach the value of 1.548 pb in our chosen parameter space. With this production rate we may discriminate models of flavor symmetry breaking and reveal a new exciting discovery channel for the signature of a single charged Higgs boson at the LHC.

ACKNOWLEDGMENTS

This work was supported in part by the National Natural Science Foundation of China, the Education Ministry of China, and a special fund sponsored by Chinese Academy of Sciences.

[1] S. L. Glashow, Nucl. Phys. **22**, 579 (1961); S. Weinberg, Phys. Rev. Lett. **19**, 1264 (1967); A. Salam, *Proceedings of the 8th Nobel Symposium Stockholm 1968*, edited by N. Svartholm (Almquist and Wiksells, Stockholm, 1968) p. 367; H. D. Politzer, Phys. Rep. **14**, 129 (1974).

[2] S. L. Glashow and S. Weinberg, Phys. Rev. D **15**, 1958 (1977).

[3] H. E. Haber and G. L. Kane, Phys. Rep. **117**, 75 (1985); J. F. Gunion and H. E. Haber, Nucl. Phys. **B272**, 1 (1986).

[4] J. F. Gunion, H. E. Haber, G. L. Kane, and S. Dawson, *The Higgs Hunter's Guide* (Addison-Wesley, Menlo Park, CA, 1990).

[5] F. Gabbiani and A. Masiero, Nucl. Phys. **B322**, 235 (1989; F. Gabbiani, E. Gabrielli, A. Masiero, and L. Silvestrini, Nucl. Phys. **B477**, 321 (1996); M. Misiak, S. Pokorski, and J. Rosiek, Adv. Ser. Dir. High Energy Phys. **15**, 795 (1998).

[6] B. Abbott *et al.* (D0 Collaboration), Phys. Rev. Lett. **82**, 4975 (1999); F. Abe *et al.* (CDF Collaboration), Phys. Rev. Lett. **79**, 357 (1997).

[7] A. A. Barrientos Bendezu and B. A. Kniehl, Nucl. Phys. **B568**, 305 (2000); O. Brein and W. Hollik, Eur. Phys. J. C **13**, 175 (2000); J. F. Gunion, H. E. Haber, F. E. Paige, W. K. Tung, and S. S. Willenbrock, Nucl. Phys. **B294**, 621 (1987); S. S. D. Willenbrock, Phys. Rev. D **35**, 173 (1987); A. Krause, T. Plehn, M. Spira, and P. M. Zerwas, Nucl. Phys. **B519**, 85 (1998).

[8] Y. Jiang, W.-G. Ma, L. Han, and Z.-H. Yu, J. Phys. G **23**, 385 (1997); **23**, 1151(E) (1997); A. Belyaev, M. Drees, O. J. P. Eboli, J. K. Mizukoshi, and S. F. Novaes, Phys. Rev. D **60**, 075008 (1999); A. Belyaev, M. Drees, and J. K. Mizukoshi, Eur. Phys. J. C **17**, 337 (2000); H.-S. Hou, W.-G. Ma, R.-Y. Zhang, Y. Jiang, L. Han, and L.-R. Xing, Phys. Rev. D **71**, 075014 (2005); S. Moretti, J. Phys. G **28**, 2567 (2002).

[9] E. Eichten, I. Hinchliffe, K. D. Lane, and C. Quigg, Rev. Mod. Phys. **56**, 579 (1984); **58**, 1065 (1986); N. G. Deshpande, X. Tata, and D. A. Dicus, Phys. Rev. D **29**, 1527 (1984); W.-G. Ma, C.-S. Li, and L. Han, Phys. Rev. D **53**, 1304 (1996); S.-H. Zhu, C.-S. Li, and C.-S. Gao, Phys. Rev. D **58**, 055007 (1998).

[10] D. A. Dicus, J. L. Hewett, C. Kao, and T. G. Rizzo, Phys. Rev. D **40**, 787 (1989); A. A. Barrientos Bendezu and B. A. Kniehl, Phys. Rev. D **59**, 015009 (1998); **63**, 015009 (2000); O. Brein, W. Hollik, and S. Kanemura, Phys. Rev. D **63**, 095001 (2001); W. Hollik and S.-H. Zhu, Phys. Rev. D **65**, 075015 (2002).

[11] J. Gunion *et al.*, Snowmass Summer Study 1990:0059-81

(QCD161:D15:1990); V. Barger, R. J. N. Phillip, and D. P. Roy, Phys. Lett. B **324**, 236 (1994); F. Borzumati, J. Kneur, and N. Polonsky, Phys. Rev. D **60**, 115011 (1999); A. Belyaev, D. Garcia, J. Guasch, and J. Solà, Phys. Lett. B **530**, 179 (2002).

[12] J. L. Diaz-Cruz, H.-J. He, and C.-P. Yuan, Phys. Lett. B **530**, 179 (2002).

[13] K. A. Assamagan, Y. Coadou, and A. Deandrea, Eur. Phys. J. direct C **4**, 1 (2002); P. Salmi, R. Kinnunen, and N. Stepanov, hep-ph/0301166; K. A. Assamagan and N. Gollub, Eur. Phys. J. C **39S2**, 25 (2005).

[14] K. A. Assamagan and Y. Coadou, Acta Phys. Pol. B **33**, 707 (2002); R. Kinnunen and A. Nikitenko, Report CMS Note No. 2003/006.

[15] S. H. Zhu, Phys. Rev. D **67**, 075006 (2003).

[16] E. L. Berger, T. Han, J. Jiang, and T. Plehn, Phys. Rev. D **71**, 115012 (2005).

[17] P. Wu, W.-G. Ma, R.-Y. Zhang, Y. Jiang, L. Han, and L. Guo, Phys. Rev. D **73**, 015012 (2006).

[18] H.-J. He and C.-P. Yuan, Phys. Rev. Lett. **83**, 28 (1999).

[19] W. Hollik, S. Penaranda, and M. Vogt, Eur. Phys. J. C **47**, 207 (2006).

[20] See, e.g, Z. Xiong and J. M. Yang, Nucl. Phys. **B628**, 193 (2002); C. Bobeth, T. Ewerth, F. Kruger, and J. Urban, Phys. Rev. D **66**, 074021 (2002); S. Rai Choudhury, Naveen Gaur, and Namit Mahajan, Phys. Rev. D **66**, 094015 (2002); **66**, 054003 (2002); S. Rai Choudhury and Naveen Gaur, Phys. Rev. D **66**, 094015 (2002); hep-ph/0205076; hep-ph/0207353.

[21] See, e.g., F. Gabbiani, E. Gabrielli, A. Masiero, and L. Silverstrini, Nucl. Phys. **B477**, 321 (1996); M. Misiak, S. Pokorski, and J. Rosiek, Adv. Ser. Dir. High Energy Phys. **15**, 795 (1998); F. Borzumati, C. Greub, and T. Hurth, Phys. Rev. D **62**, 075005 (2000); T. Besmer, C. Greub, and T. Hurth, Nucl. Phys. **B609**, 359 (2001).

[22] M. J. Duncan, Nucl. Phys. **B221**, 285 (1983); Phys. Rev. D **31**, 1139 (1985).

[23] K. Hikasa and M. Kobayashi, Phys. Rev. D **36**, 724 (1987).

[24] T. P. Cheng and M. Sher, Phys. Rev. D **35**, 3484 (1987).

[25] See, e.g., S. Dimopoulos and D. Sutter, Nucl. Phys. **B452**, 496 (1995); F. Gabbiani, *et al.*, Nucl. Phys. **B477**, 321 (1996); M. Misiak, S. Pokorski, and J. Rosiek, Adv. Ser. Dir. High Energy Phys. **15**, 795 (1998).

[26] H. L. Lai *et al.* (CTEQ Collabroation), Eur. Phys. J. C **12**, 375 (2000).

[27] A. Denner, Fortschr. Phys. **41**, 307 (1993).

[28] M. Carena, D. Garcia, U. Nierste, and C. E. Wagner, Nucl. Phys. **B577**, 88 (2000).

[29] S. Dawson, C. B. Jackson, L. Reina, and D. Wackeroth, Phys. Rev. D **69**, 074027 (2004).

[30] L. J. Hall, R. Rattazzi, and U. Sarid, Phys. Rev. D **50**, 7048 (1994); R. Hempfling, Phys. Rev. D **49**, 6168 (1994); M. Carena, M. Olechowski, S. Pokorski, and C. E. M. Wagner, Nucl. Phys. **B426**, 269 (1994); D. Pierce, J. Bagger, K. Matchev, and R. Zhang, Nucl. Phys. **B491**, 3 (1997).

[31] J. Guasch, P. Häfliger, and M. Spira, Phys. Rev. D **68**, 115001 (2003).

[32] P. Häfliger and M. Spira, Nucl. Phys. **B719**, 35 (2005).

[33] L. Reina, S. Dawson, and D. Wackeroth, Phys. Rev. D **65**, 053017 (2002).

[34] W. Beenakker, R. Höpker, and P. M. Zerwas, Phys. Lett. B **378**, 159 (1996); W. Beenakker, R. Höpker, T. Plehn, and P. M. Zerwas, Z. Phys. C **75**, 349 (1997).

[35] W. T. Giele and E. W. N. Glover, Phys. Rev. D **46**, 1980 (1992); W. T. Giele, E. W. Glover, and D. A. Kosower, Nucl. Phys. **B403**, 633 (1993); S. Keller and E. Laenen, Phys. Rev. D **59**, 114004 (1999).

[36] S. Eidelman *et al.*, Phys. Lett. B **592**, 1 (2004).

[37] B. C. Allanach *et al.*, Eur. Phys. J. C **25**, 113 (2002); B. C. Allanach *et al.*, in *Proceedings of APS/DPF/DPB Summer Study on the Future of Particle Physics (Snowmass 2001), Snowmass, Colorado*, eConf C010630 (2001) p. 125.

[38] Nabil Ghodbane and Hans-Ulrich Martyn, hep-ph/0201233.

[39] H. Baer *et al.*, hep-ph/0001086.

[40] N. Ghodbane *et al.*, hep-ph/9909499.

[41] T. Sjöstrand *et al.*, hep-ph/0108264.